TESTING OF TIMBER-TO-TIMBER SCREW-CONNECTIONS IN HYBRID CONFIGURATIONS

Authors: Gianni Schiro, Ivan Giongo, Wendel Sebastian, Daniele Riccadonna and Maurizio Piazza

Corresponding author: Maurizio Piazza maurizio.piazza@unitn.it

---

ABSTRACT

This paper presents the results of an extensive experimental study on the short-term mechanical performance of timber screw connections comprising different types of fasteners (inserted at 45° and 90° to the grain) and different timber products (solid sawn timber, glued laminated timber, cross laminated timber and laminated veneer lumber) made from both softwood and hardwood species. Fifty eight specimens laid out in fourteen arrangements were tested under quasi-static monotonic loading. The test configurations were meant to reproduce connections used in timber-to-timber hybrid composite structures for applications in both new constructions and retrofit interventions. Result comparisons regarding connection stiffness, strength, static ductility, residual strength and failure mode are presented and discussed. Additionally, the experimental data are used to check the extents of validity of existing analytical approaches (mainly developed for softwoods) to screw connections comprising hardwood elements. Practical aspects concerning screw insertion into hardwood elements are also addressed within the paper.

KEYWORDS: Hybrid structures, hardwood, beech LVL, timber composite floors, timber connections, inclined screws.

---

1 INTRODUCTION

Several typologies of self-tapping screws (for use in timber constructions) covering a wide variety of structural applications have been developed over the past two decades and are currently available on the market ([1]). A possible way to classify them can be to refer to the fastener threaded part. Three main classes can be identified, namely partially threaded screws (also referred to as single-threaded screws, ST), double threaded screws (DT) and fully-threaded screws (FT, also referred to as all-threaded screws). There are also screws that do not neatly fit into either of these three categories, as they are designed for special purposes like coupling timber with other materials, such as concrete or steel. In contrast to other connector types (e.g. lag screws), there is currently no harmonized standard that establishes the requirements for structural screws. Consequently, each of the three classes (ST, DT and FT) includes fasteners that differ from each other for thread, head and tip geometry. The mechanical properties are provided by the producers in the product standards (e.g. European Technical Assessment, ETA: [22], [23], [24] and [25]).

It is evident that when such connectors are used in configurations that are not specifically described by the product standards, their performance needs to be evaluated experimentally [2]. Extrapolation of the results from other “similar” fastener types is inadvisable, unless these extrapolations are proof-checked by testing. For example, in Eurocode 5 [15] it is advised that the slip modulus of a timber-concrete connection is taken as double the value of the modulus calculated by means of the formula given for a parallel timber-timber connection. That is because an approach has not yet been developed specifically for timber-concrete connections. Hence, in the status quo, these timber-timber extended predictions are backed up by tests on the timber-concrete connections under consideration.

The present paper focuses on connection configurations that are intended for use in the field of timber-to-timber composite structures where the fasteners may be inserted at an angle to the grain other than 90° and may connect different timber products (e.g. solid sawn timber with cross laminated timber) and/or elements from different timber species (e.g. softwood elements with hardwood elements). Extensive details on the tested configurations and the purposes they are designed for, will be provided in section 2.

Structural solutions in which DT and FT screws are loaded in a combination of shear and tension are becoming more common. Interesting studies into the mechanical performance of such connections (softwood) can be found in the literature ([3] and [4]), where formulations to evaluate connection strength and stiffness are also proposed. However, to the best of the authors’ collective knowledge there are no data available on ST screws loaded in a shear-tension configuration, despite available evidence of applications showing advantages from such use [5].

The optimization/specialization process that leads to widening of the timber fastener range also involves timber as a construction material. Wood based structural products now include solid sawn timber, glued-laminated timber, laminated veneer lumber and cross-laminated timber. “New” wood species (such as poplar, oak, birch and beech) are being actively considered for structural purposes by the construction industry (see [6], [7] and [8]) and will soon compete with the traditional (for construction) softwood species (e.g. pine, spruce, larch).

This will only be really possible once the performance of mechanical connections realized with these new products (often characterized by very high density values) has been thoroughly investigated and sound analytical formulations to predict their behavior have been developed.

Studies including [9] – [12] have provided first insights that will help close the gap between the availability of new engineered components in renewable materials with high mechanical performance and the wide application of these components in real construction projects.

In the following sections of this paper, the outcomes of an extensive experimental campaign on short-term testing of timber screw-connections comprising specimens realized with multiple combinations of timber products, screw types and screw configurations, will be presented. The specimens and tests are first described, following which interpretation of the results to infer connection properties on strength, stiffness and ductility will be presented. Finally, conclusions are drawn.

2 CONNECTION TESTS

2.1 TEST CONFIGURATION AND GEOMETRY

The experimental campaign was carried out at the laboratory of the Department of Civil, Environmental and Mechanical Engineering (DICAM) of the University of Trento and totalled 58 pushout tests covering 14 configurations. Different solutions were investigated in order to characterise the mechanical behaviour, in terms of stiffness, strength, static ductility and residual strength of connections mainly designed for the realisation of timber-to-timber composite (TTC) floors. The significant parameters that describe the tested samples, such as geometry, materials and joint configuration, are reported in Table 2-1. Note that, within specimens where the screws were inclined at 45°, all screws were parallel to each other (not in an X-formation) to enable exploitation of the beneficial orientation of the screws (shear-tension configuration). As shown in Figure 2-3, the double-shear specimen layouts used during the tests are those commonly employed in pushout tests and consist of a central timber element flanked by two side elements symmetrically disposed. As will be specified hereinafter, for some tests an interlayer element made of timber boards was added. This represented the situation where timber reinforcing elements are positioned on the existing flooring, a common practice in retrofit interventions. Consistently with EN 1995-1-1 [15], the samples were designed in order to avoid failures strictly related to inadequate screw spacing and distances from the edges.

Table 2-1 Test configurations

Test		App.	Central element	Interlayer	Side elements		Connections		
ID	n°		Type	t_i [mm]	Type	t_s [mm]	Type	Washer	α
PA	4	N	Beech LVL beam	-	CLT panel	57	DT$_A$ 8.5x150	-	45°
PB	4	N	Beech LVL beam	-	CLT panel	57	ST$_A$ 10x220	W+GC	45°
PC	4	N	Beech LVL beam	-	Beech LVL panel	40	ST$_A$ 10x160	W+GC	45°
PD	5	N	Beech LVL beam	-	Beech LVL panel	40	ST$_A$ 10x220	SW	45°
PE	5	N	Beech LVL beam	-	Beech LVL panel	40	ST$_A$ 10x220	W	90°
PF	5	R	Spruce Solid wood	20	Beech LVL on its side	50	ST$_A$ 10x220	W+GC	45°
PG	2	R	Spruce Solid wood	20	Beech LVL on its side	50	ST$_A$ 10x220	GC	45°
PH	3	R	Spruce Solid wood	20	Beech LVL on its side	50	DT$_A$ 8.5x190	-	45°
PI	3	N	Spruce Solid wood	-	CLT panel	57	DT$_A$ 8.5x150	-	45°
PL	3	N	Spruce Solid wood	-	CLT panel	57	ST$_A$ 10x220	W+GC	45°
PM	5	R	Spruce Solid wood	20	CLT panel	57	DT$_B$ 8.2x190	-	45°
PN	5	R	Spruce Solid wood	20	CLT panel	57	ST$_B$ 10x200	W+GC	45°
PO	5	R	Spruce Solid wood	20	CLT panel	57	ST$_B$ 10x200	W	90°
PP	5	R	Spruce Solid wood	20	CLT panel	57	ST$_B$ 10x200	-	90°

Note:
n°: Number of repetitions
R: Retrofit application
GC: Groove cut
App.: Application
W: Washer
SW: Special washer
N: New application
ST: Single threaded screw
DT: Double threaded screw

Essentially, the aims of the experimental campaign were two-fold. The first goal was to investigate the mechanical behaviour of connections specifically designed for newly constructed high-performance TTC floors. Hybrid solutions, that coupled the lightness of softwood elements (spruce cross laminated panels), with the strength of hardwood components (beech laminated veneer lumber beams/panels) by means of different types of connectors (tests PA and PB), were compared with “more common” timber-to-timber solutions (tests PI and PL). In addition, hardwood-hardwood configurations were studied (tests PC, PD and PE).

The second goal was to evaluate the performance of connections designed for retrofit solutions on existing timber floors. In order to reproduce realistic scenarios present in historical buildings, only solid wood elements made of spruce were used for the central part of the specimens (instead of using for example glulam). As stated earlier, timber boards were inserted between the central and side elements to simulate an existing flooring. As regards the reinforcing elements (corresponding to the lateral elements of the samples), two different solutions were adopted: softwood cross laminated panels (tests PM, PN, PO and PP) and beech LVL beams arranged on their side (tests PF, PG and PH). The use of a slender beam element with a reduced section instead of a panel enables enhanced out-of-plane performance of timber diaphragms in case of large deformations or where adjacent existing joists exhibit different levels of sagging.

2.2 TIMBER ELEMENTS

Different timber products obtained from different both softwood and hardwood species were employed in the experimental campaign. For the central components, spruce solid wood graded as strength class C24 [19] and beech laminated veneer lumber (LVL) of grade GL70 [18] were considered. Two types of panel were selected for the side elements: three-layer cross laminated timber (CLT) of 57 mm thickness [21] and beech LVL (w/o cross layers) of 40 mm thickness [20]. In addition, to simulate a further retrofit solution, beech LVL beams (GL70) arranged on their side were used. The mechanical properties and the density (from product documentation and experimental data) of the various elements are reported in Table 2-2.

Table 2-2 Strength and stiffness properties for timber elements

Element type and grading			Beech LVL GL70 [18]	Spruce Solid wood C24 [19]	Beech LVL panel [20]	Spruce CLT panel [21]
Bending:	$f_{m,k}$	[MPa]	70	24	80	24
Tension:	$f_{t,0,k}$	[MPa]	55	19.2	60	14
	$f_{t,90,k}$	[MPa]	0.6	0.5	1.5	0.12
Compression:	$f_{c,0,k}$	[MPa]	59.4	24	57.5	21
	$f_{c,90,k}$	[MPa]	10.2	2.5	14	2.5
Shear:	$f_{v,k}$	[MPa]	4	3.5	8	3.3
Mean modulus:	$E_{0,mean}$	[MPa]	16700	11500	16800	12000
Density:	ρ_{mean}	[kg/m^3]	≥ 740	420	800	450-500
Density (experimental):	$\rho_{experim..}$ CoV	[kg/m^3]	796 0.7%	460 2.7%	846 0.5%	465 1.2%

From Table 2-2 it is possible to note that beech LVL panel has better mechanical properties than beech LVL GL70 (with the exception of compression parallel to the grain) despite both being made of beech laminated veneers. Such difference is to be attributed, at least partly, to the different veneer thickness (*4 mm* for GL70 beams and *3 mm* for LVL panels).

2.3 CONNECTORS

The fasteners employed in the experimental campaign (Figure 2-1) belong to two macro groups: single (or partially) threaded screws (ST_A [22] and ST_B [23]) and double threaded screws (DT_A [24] and DT_B [25])

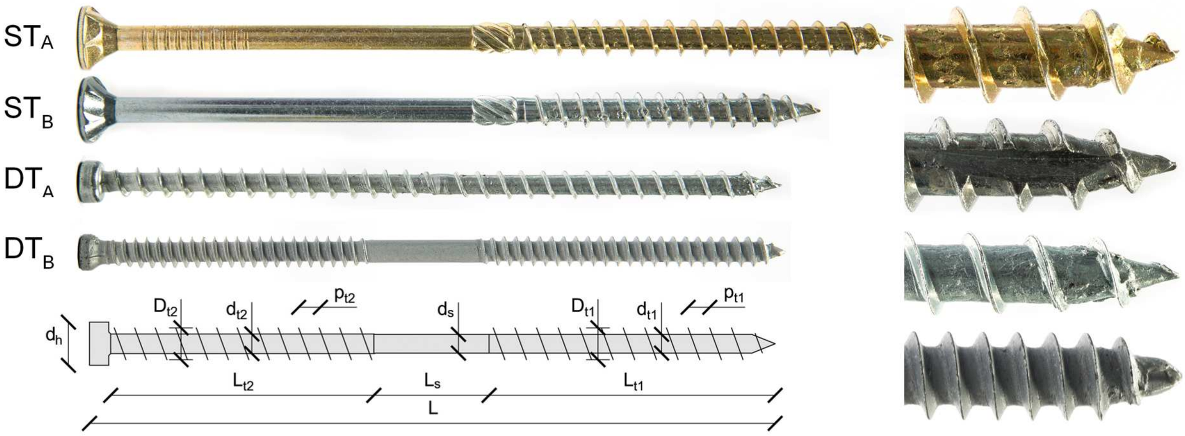

Figure 2-1 Screw types

The geometries of the ST screws were quite similar to each other, with a countersunk head and a milling cutter between the thread and the shank. The main difference between ST$_A$ and ST$_B$ fasteners lies in the shape of the tip, with a pronounced cutter on the tip of ST$_B$.

As regards the DT connectors, the different diameters (D_{t1} and D_{t2}) and pitches (p_{t1} and p_{t2}) of the two threaded parts, are optimised to generate a pulling and closing effect in the joint. DT$_B$ screws are characterised by a clearly-distinguishable smooth part at the screw mid-length (L_s) and a cylindrical head having a diameter (D_h) comparable with D_{t2} (Table 2-3). Differently, DT$_A$ screws have a shorter central smooth part (L_s), a bigger head diameter (D_h) and considerably larger pitches (p_{t1} and p_{t2}).

The dimensions (Figure 2-1) and the mechanical properties provided by the relevant European Technical Approval (ETA) are summarised in Table 2-3.

Table 2-3 Connector geometry and properties

Connector:		ST$_A$ [22]		ST$_B$ [23]	DT$_A$ [24]		DT$_B$ [25]
L	[mm]	220	160	200	190	150	190
L_{t1}	[mm]	100	100	80	90	70	80
d_{t1}	[mm]	6.3	6.3	6.4	5.3	5.3	5.4
D_{t1}	[mm]	10	10	10	8	8	8.2
p_{t1}	[mm]	6.6	6.6	5.4	6	6	3.2
L_s	[mm]	120	60	120	5	5	30
d_s	[mm]	7.2	7.2	7	5.6	5.6	6.3
L_{t2}	[mm]	-	-	-	90	70	80
d_{t2}	[mm]	-	-	-	5.025	5.025	5.4
D_{t2}	[mm]	-	-	-	8.5	8.5	8.9
p_{t2}	[mm]	-	-	-	5.68	5.6	3
d_h	[mm]	18.5	18.5	18.25	12	12	10
$M_{y,k}$	[Nm]	36	36	36	20	20	19.5
$f_{y,k}$	[Mpa]	600	600	600	900	900	870
$R_{tens,k}$	[kN]	26	26	31.4	18	18	28.6
$f_{tor,k}$	[Nm]	45	45	40	23	23	25.9

Where $M_{y,k}$ is the characteristic yield moment, $f_{y,k}$ is the characteristic yield strength, $R_{tens,k}$ is the characteristic tensile strength, $f_{tor,k}$ is the characteristic torsional strength and $f_{head,k}$ is the characteristic strength of the screw head.

As supplied by the producers, washers with different geometries were adopted. In particular, ST_A screws were coupled with the washers shown in Figure 2-2-C (top) and ST_B screws with the washers reported in Figure 2-2-C (bottom). The first type of washers is characterised by a thin section with a countersunk bottom surface, while the second type has a squatter, more compact structure with a totally flat surface at the bottom.

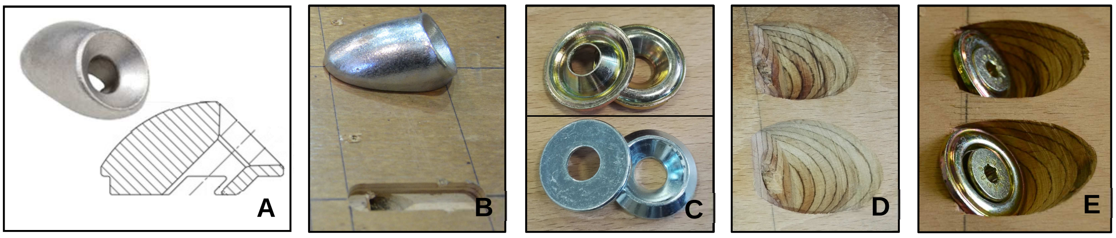

Figure 2-2 Washers and groove cuts

For the configurations where the single threaded screws were inserted at an angle (α) different from 90°, groove cuts (GC, Figure 2-2-D) were prepared prior to the assembly of the samples in order to have a wider contact area between the wood and the washer (Figure 2-2-E).

For timber-to-timber hybrid retrofit solutions (where softwood joists are coupled with hardwood reinforcing elements), samples without washers were also tested to verify the necessity of using washers. This additional solution was considered bearing in mind that, because of the high density of wood (see Table 2-2) under the screw heads, failure is determined by thread withdrawal from the softwood element.

As previously mentioned, the washers for single threaded screws that are available on the market, are usually designed for a 90° configuration. As an alternative solution to the groove cuts, the use of washers with a modified geometry could facilitate the assembly operations. However, due to the lack of washers designed ad hoc for timber-to-timber joints with inclined screws, special washers (SW, Figure 2-2-A and Figure 2-2-B) that are designed for steel-to-timber connections were employed. As shown in Figure 2-2-B, a groove cut was nonetheless necessary due to the shape of the bottom surface of the SW. As will be discussed hereinafter, the design of an optimised washer could result in the complete elimination of groove cuts.

Regarding the double threaded screws selected for the tests, the following remarks can be reported: DT_A screws compared to DT_B screws are characterised by a wider pitch for each thread, a shorter smooth part of the shank and a larger diameter of the head (see Figure 2-1 and Table 2-3).

2.4 TEST SETUP AND INSTRUMENTS

Every test specimen was subjected to quasi-static monotonic loading. According to EN 12512 [16], the constant rate of slip was set equal to 0.05 mm/s (a range between 0.02 mm/s and 0.2 mm/s is recommended by [16]). The setup was designed to allow maximum displacement values up to 100 mm. Although a slip limit of 30 mm is considered as ultimate condition by [16], where possible, the specimens were pushed up to their actual failure limit state in order to evaluate the residual capacity also for high values of displacement.

The load, introduced by a universal testing machine (Figure 2-3) through a hydraulic actuator, was monitored with a 1000 kN load cell (the values of maximum forces range in the field 80 – 360 kN). Two linear variable differential transformer transducers (LVDTs) were employed (sensitivity of 2 mV/V) to measure the slip between the central and side elements. A further inductive transducer was introduced to provide alternative measures of the total vertical displacement. The recording was done continuously with a frequency rate of 2 Hz via a multi-channel data recording device.

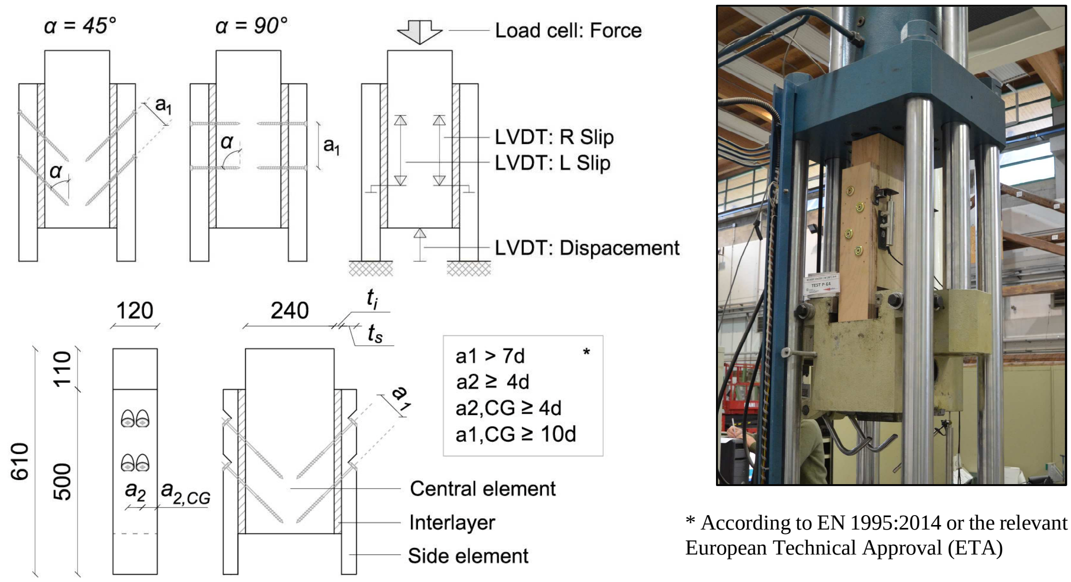

* According to EN 1995:2014 or the relevant European Technical Approval (ETA)

Figure 2-3 Specimen geometry and test setup

2.5 ESTIMATION OF CONNECTION MECHANICAL PARAMETERS

The standards adopted as reference for the evaluation of the connection performance parameters (yield point, secant stiffness, ultimate conditions and static ductility) were EN 12512 [16] and EN 26891 [17].

The slip modulus K_s of the connections (corresponding to the slip modulus K_{ser} provided by EN 1995-1-1 [15]) can be calculated by means of the following equation [17]:

$$K_s = \frac{0.4\,F'_{\mathrm{max}} - 0.1\,F'_{max}}{v_{0.4} - v_{0.1}} \tag{1}$$

where $v_{0.1}$ and $v_{0.4}$ are the connection slips (evaluated for each specimen) corresponding to loading equal to $0.1 \cdot F'_{max}$ and $0.4 \cdot F'_{max}$ respectively; F'_{max} is the mean value of the maximum force values $F'_{max,i}$ registered for all test repetitions associated with each configuration (consistently with EN 26891 [17], excluding values that deviated by more than 20% from the mean). For each test, $F'_{max,i}$ is equal to the actual maximum load $F_{max,R}$ when the corresponding slip value was less than 15 mm, otherwise the load corresponding to a 15 mm slip F_{15} was used [17].

According to [16], the yield point (F_y, v_y) is determined as shown in Figure 2-4. In particular, case A refers to a load-slip curve with two well-defined linear parts, while case B refers to a curve with a pronounced non-linear behaviour. Case C is added to represent tests with a linear-elastic behaviour up to the maximum load.

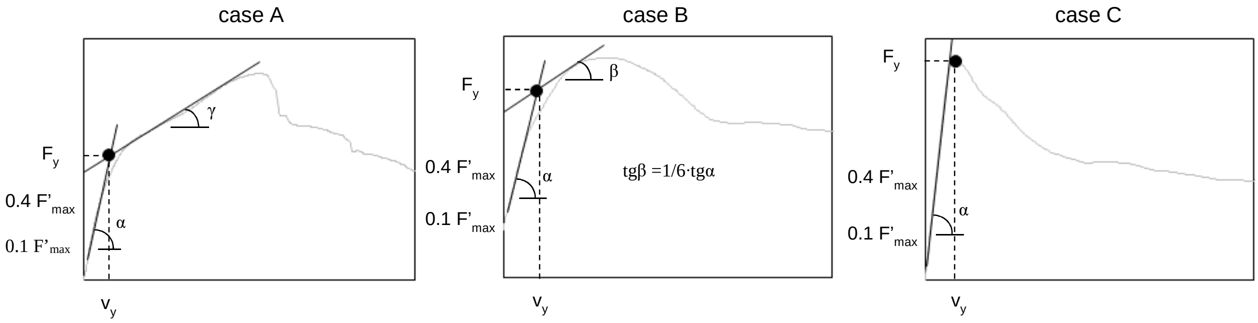

Figure 2-4 Definition of yield point for a load-slip (F-v) curve

The ultimate slip v_u corresponds to the first of the following conditions: failure of the specimen, slip at 0.8 times $F_{max,R}$ on the descending branch and a slip value of 30 mm [16]. The ductility D is calculated as the ratio between ultimate slip and yield slip according to [16].

2.6 EXPERIMENTAL RESULTS

In Figure 2-5 the experimental results from each configuration tested are plotted in terms of connection shear force (per single fastener) versus slip (average value from both specimen sides). The red curve in each diagram represents the mean curve of all measured force-slip curves.

Consistently with section 2.5, the connection performance parameters (maximum load, slip modulus, yield point and ductility) that were derived from the test data, are also reported in Figure 2-5. For every parameter, the coefficient of variation (*CoV*), is given.

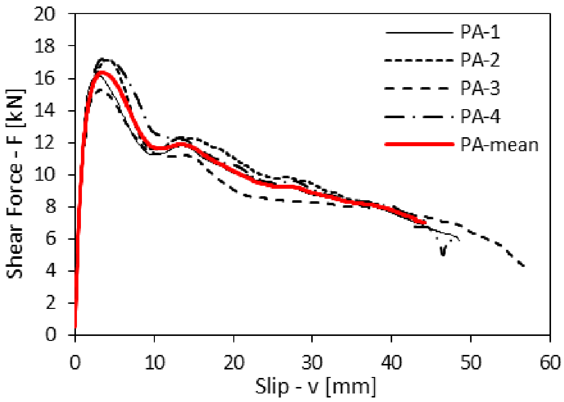

Test PA		Mean	CoV
$F_{max,R}$	[kN]	16.35	4.5%
K_s	[N/mm]	13234	3.4%
F_y	[kN]	12.98	4.8%
v_y	[mm]	0.91	9.2%
D		8.53	14.8%

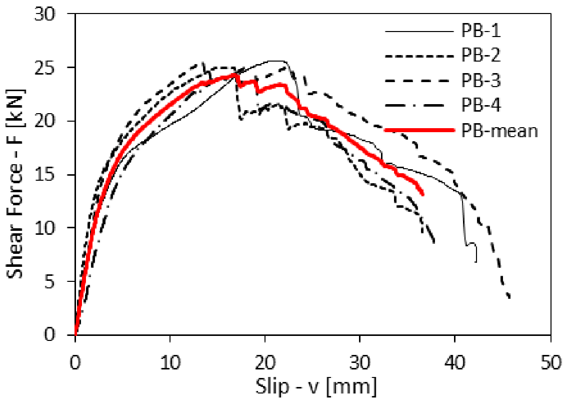

Test PB		Mean	CoV
$F_{max,R}$	[kN]	25.34	1.1%
K_s	[N/mm]	5369	23.8%
F_y	[kN]	16.13	8.1%
v_y	[mm]	3.26	29.0%
D		7.76	19.1%

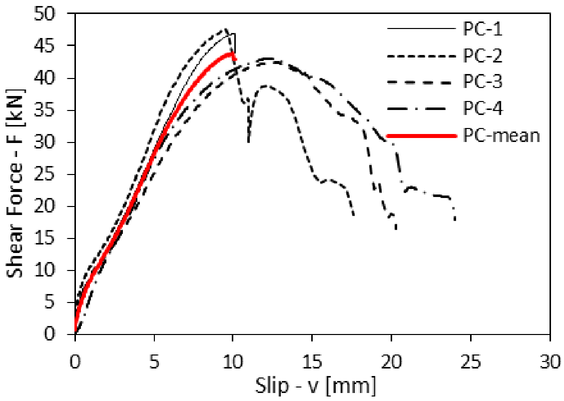

Test PC		Mean	CoV
$F_{max,R}$	[kN]	44.95	5.0%
K_s	[N/mm]	4924	7.3%
F_y	[kN]	42.86	8.2%
v_y	[mm]	8.20	6.7%
D		-	-

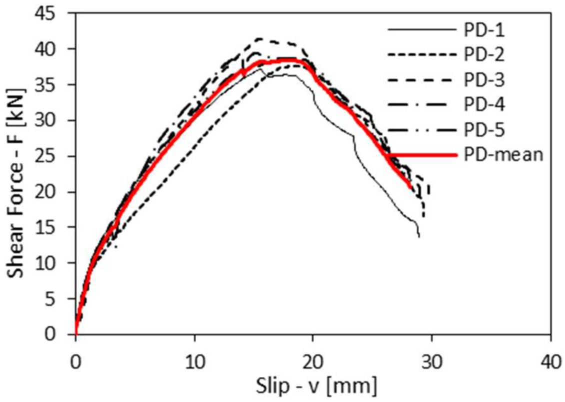

Test PD		Mean	CoV
$F_{max,R}$	[kN]	38.91	3.9%
K_s	[N/mm]	4192	17.9%
F_y	[kN]	20.46	17.0%
v_y	[mm]	4.54	24.2%
D		5.33	17.3%

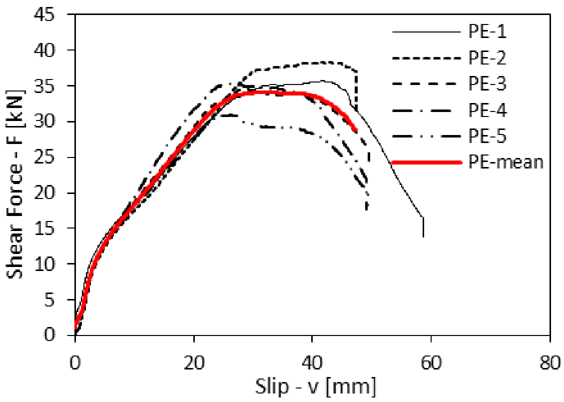

Test PE		Mean	CoV
$F_{max,R}$	[kN]	35.03	6.8%
K_s	[N/mm]	3035	13.6%
F_y	[kN]	12.38	7.8%
v_y	[mm]	4.12	9.1%
D		7.35	8.9%

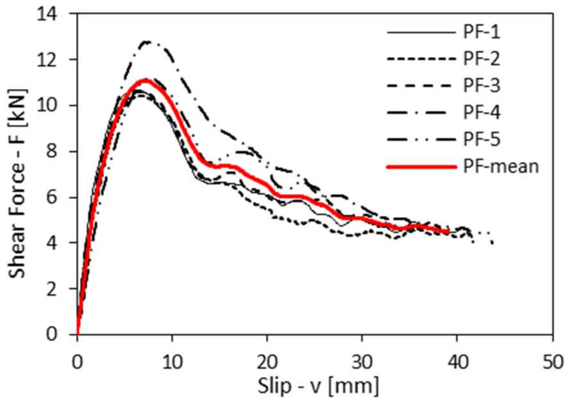

Test PF		Mean	CoV
$F_{max,R}$	[kN]	11.13	7.6%
K_s	[N/mm]	3332	16.7%
F_y	[kN]	9.36	6.6%
v_y	[mm]	2.91	22.7%
D		4.09	18.5%

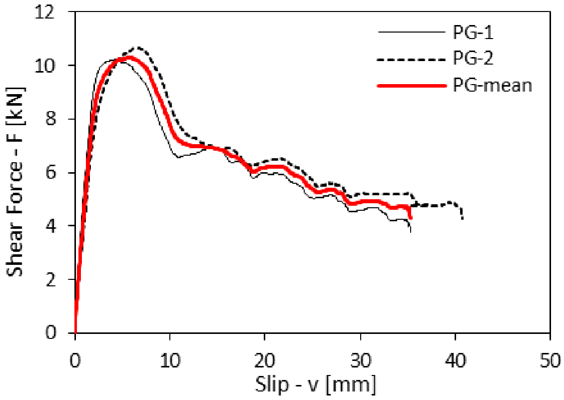

Test PG		Mean	CoV
$F_{max,R}$	*[kN]*	10.45	2.2%
K_s	*[N/mm]*	4472	14.9%
F_y	*[kN]*	9.01	2.6%
v_y	*[mm]*	1.93	12.8%
D		4.85	5.1%

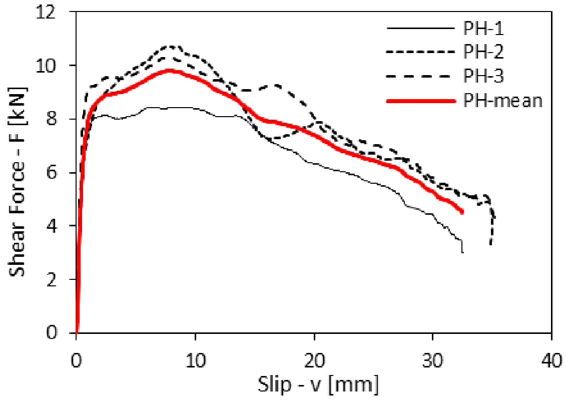

Test PH		Mean	CoV
$F_{max,R}$	*[kN]*	9.83	10.1%
K_s	*[N/mm]*	13468	20.6%
F_y	*[kN]*	8.59	6.2%
v_y	*[mm]*	0.66	12.5%
D		27.01	24.1%

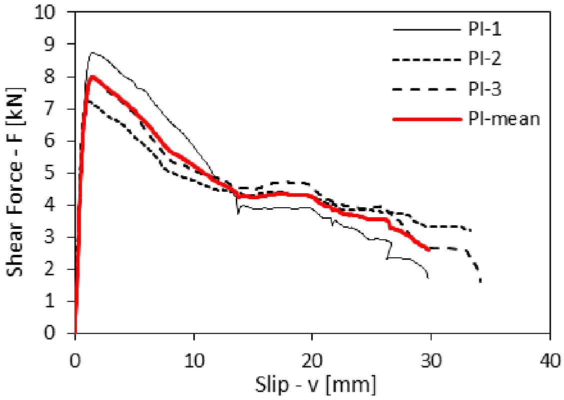

Test PI		Mean	CoV
$F_{max,R}$	*[kN]*	8.00	7.8%
K_s	*[N/mm]*	9773	12.8%
F_y	*[kN]*	8.00	7.8%
v_y	*[mm]*	1.36	13.0%
D		4.74	14.4%

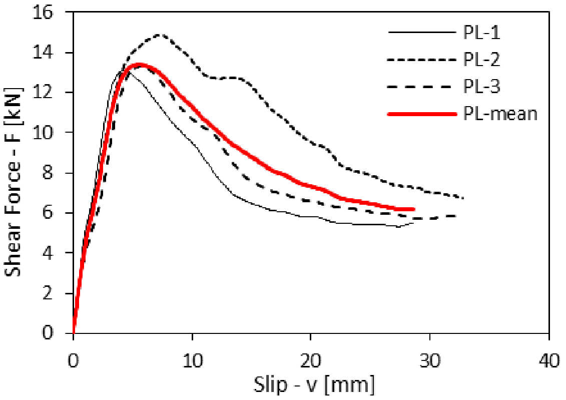

Test PL		Mean	CoV
$F_{max,R}$	*[kN]*	13.75	5.7%
K_s	*[N/mm]*	3744	20.3%
F_y	*[kN]*	12.59	3.4%
v_y	*[mm]*	3.45	23.3%
D		3.45	32.1%

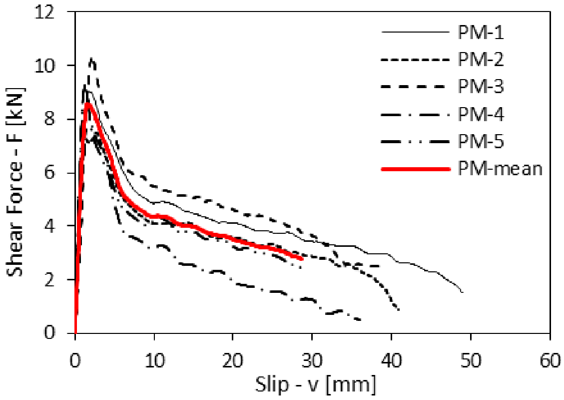

Test PM		Mean	CoV
$F_{max,R}$	*[kN]*	9.06	10.0%
K_s	*[N/mm]*	7835	28.4%
F_y	*[kN]*	9.06	10.0%
v_y	*[mm]*	1.86	27.5%
D		1.96	11.0%

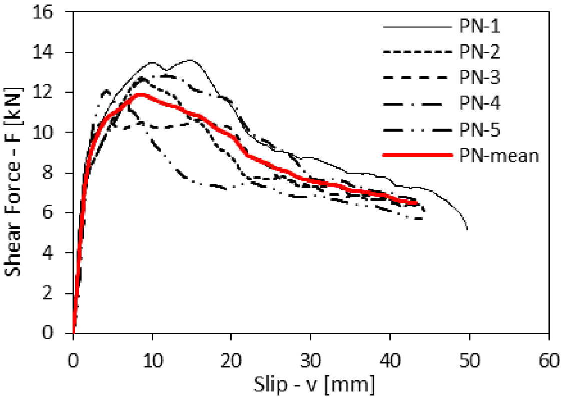

Test PN		Mean	CoV
$F_{max,R}$	*[kN]*	12.37	8.0%
K_s	*[N/mm]*	5700	12.4%
F_y	*[kN]*	8.90	12.3%
v_y	*[mm]*	1.68	23.6%
D		12.02	34.3%

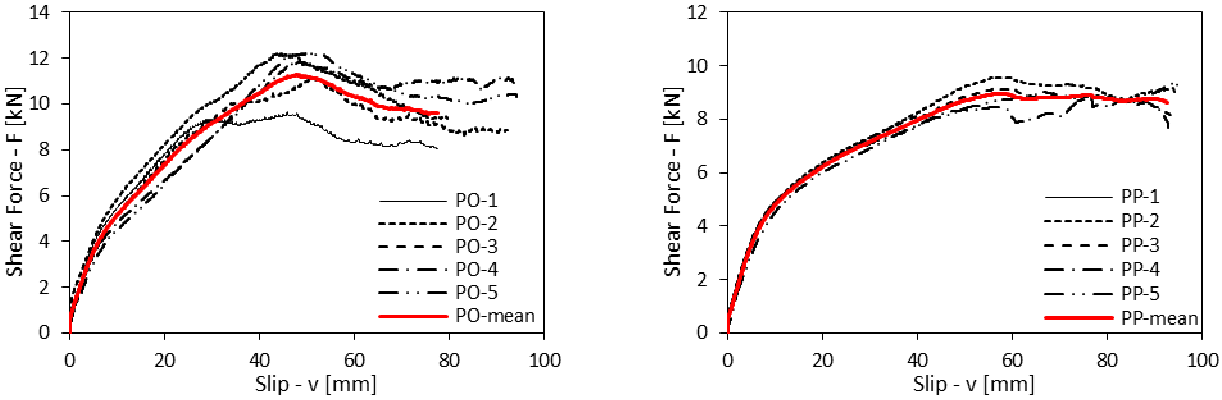

Test PO		Mean	CoV
$F_{max,R}$	*[kN]*	11.41	8.5%
K_s	*[N/mm]*	749	22.6%
F_y	*[kN]*	4.02	9.3%
v_y	*[mm]*	4.94	13.8%
D		6.19	13.1%

Test PP		Mean	CoV
$F_{max,R}$	*[kN]*	9.22	3.0%
K_s	*[N/mm]*	616	11.8%
F_y	*[kN]*	4.91	3.5%
v_y	*[mm]*	7.57	16.6%
D		4.07	15.8%

Figure 2-5 Experimental results

For the sake of comparison, all the experimental results in terms of maximum load ($F_{max,R}$) and slip modulus (K_s), are summarised in Figure 2-6. As will be better described in the comparison paragraphs (see section 3), DT screws generally exhibited higher values of stiffness than ST screws, while joints realized with hardwood (especially those where the central element is made of hardwood) resulted in higher connection capacity values when compared to joints where softwood was used.

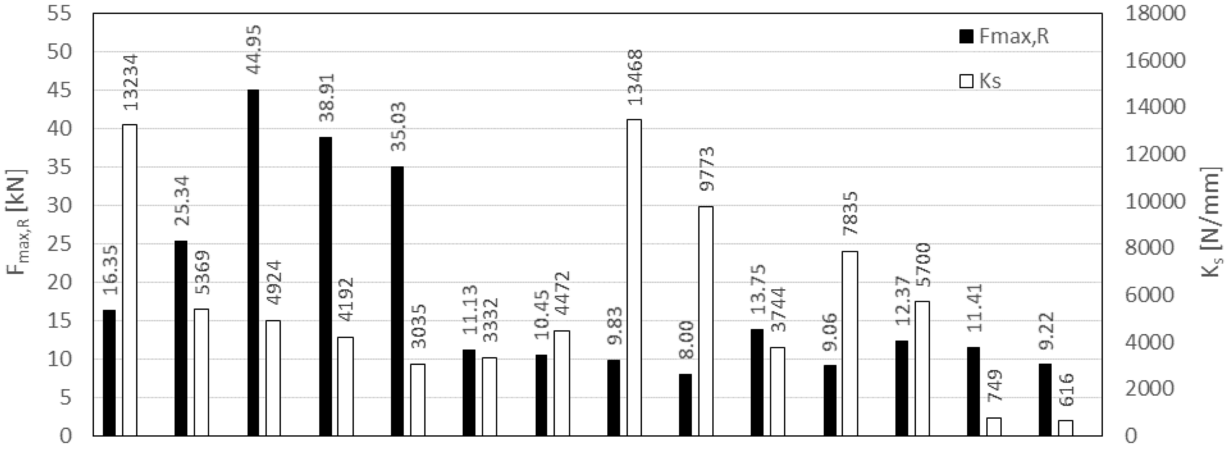

	P-A	P-B	P-C	P-D	P-E	P-F	P-G	P-H	P-I	P-L	P-M	P-N	P-O	P-P
C. element	▨	▨	▨	▨	▨	☐	☐	☐	☐	☐	☐	☐	☐	☐
S. element	☐	☐	▨	▨	▨	▨	▨	▨	☐	☐	☐	☐	☐	☐
Screw	DT_A	ST_A	ST_A	ST_A	ST_A	ST_A	ST_A	DT_A	DT_A	ST_A	DT_B	ST_B	ST_B	ST_B
L_{screw} [mm]	150	220	160	220	220	220	220	190	150	220	190	200	200	200
α	45°	45°	45°	45°	90°	45°	45°	45°	45°	45°	45°	45°	90°	90°
Washer	-	W +GC	W +GC	SW	W	W +GC	GC	-	-	W +GC	-	W +GC	W	-
Interlayer	-	-	-	-	-	20	20	20	-	-	20	20	20	20

☐ Softwood ▨ Hardwood

Figure 2-6 Experimental results in terms of maximum load and slip modulus

2.7 COMPARISON BETWEEN EXPERIMENTAL RESULTS AND THEORETICAL MODELS

In this section, the experimental results in terms of connection capacity and slip modulus are compared to the values predicted by means of theoretical models available in literature.

The characteristic load-bearing capacity ($F_{max,k,th}$) of dowel type connectors subjected to shear loading (α=90°) can be calculated by using the theoretical model included in the EN 1995-1-1 [15], which is based on Johansen theory [14]. For fasteners inserted at an angle α with respect to the shear plane (0°≤ α ≤90°), a theoretical model for the estimation of the connection capacity was proposed by Bejtka and Blaß in [3]. In this model, the ultimate load of the joints is related not only to the bending strength of the connectors and the embedment strength of the wood elements as in [15], but also to the axial capacity of the fasteners and the friction forces between the timber elements. The different failure modes expected for the configurations where 0°≤ α ≤90°, are illustrated in Figure 2-7.

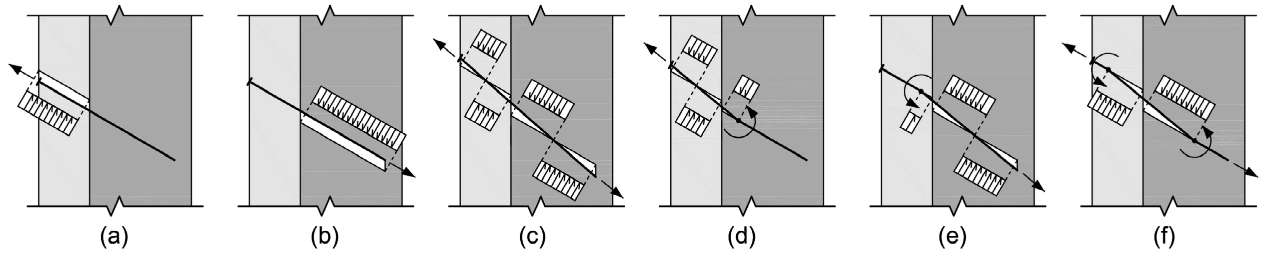

Figure 2-7 Failure modes for inclined fasteners

The theory proposed by Bejtka and Blaß in [3] was applied adopting the following assumption: for those modes where the failure mechanism is mainly governed by the strength properties of just one of the two timber elements (i.e. modes *a, b, d, e*), the axial capacity of the fastener was calculated by considering only the screw-portion within the “actively involved element”. More details on the equations and the parameters used to calculate the theoretical load-bearing capacity are provided in the Annex A to the document.

Sensitivity analysis showed negligible sensitivity of the predicted capacity values to small variations (5% - 10%) in timber density and screw yield moment, compatible with observed differences between the experimentally measured parameters and the values provided by product certificates.

By applying the aforementioned theoretical approach, characteristic values (5% percentile) of the connection strength were determined ($F_{max,k,th}$). The characteristic values of the experimental yield strength ($F_{y,k,exp}$) and maximum capacity ($F_{max,k,exp}$), were determined in accordance with Annex D of EN 1990 [26]. The values reported in Figure 2-8 were determined under the following hypotheses: log-normal distribution of the data and coefficient of variation not known from prior knowledge. In cases where the coefficient of variation is not known from prior knowledge, a minimum number of three specimens should be adopted in order to identify the reference log-normal distribution [26]. It is worth mentioning that due to malfunctioning of the data acquisition system, it was not possible to record the results from specimen PG-3 and that means that only two test repetitions were available for PG test type. Consequently, for comparison purpose, the log-normal distribution was determined nonetheless, by adopting the characteristic fractile factor provided by [26] for three-specimen samples. A comparison between the predicted values and the experimental results is reported in Figure 2-8.

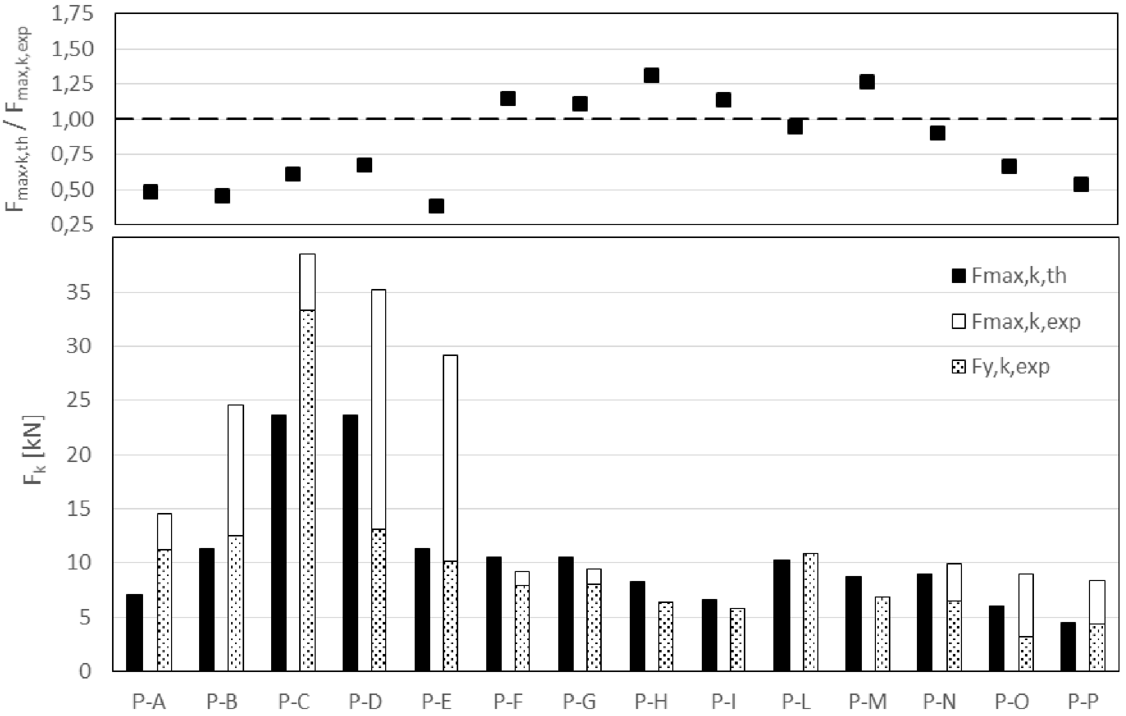

	P-A	P-B	P-C	P-D	P-E	P-F	P-G	P-H	P-I	P-L	P-M	P-N	P-O	P-P
C. element	▨	▨	▨	▨	▨	☐	☐	☐	☐	☐	☐	☐	☐	☐
S. element	☐	☐	▨	▨	▨	▨	▨	▨	☐	☐	☐	☐	☐	☐
Screw	DT_A	ST_A	ST_A	ST_A	ST_A	ST_A	ST_A	DT_A	DT_A	ST_A	DT_B	ST_B	ST_B	ST_B
α	45°	45°	45°	45°	90°	45°	45°	45°	45°	45°	45°	45°	90°	90°
Failure *	a	a	a	a	d	f	f	f	b	f	b	f	f	f
$F_{max,k,th}$ [kN]	7,06	11,28	23,61	23,61	11,29	10,49	10,49	8,32	6,59	10,32	8,73	8,98	5,97	4,50
$F_{max,k,exp}$ [kN]	14,52	24,50	38,53	35,20	29,14	9,17	9,43	6,36	5,77	10,90	6,88	9,94	9,02	8,40

* Failure mode according to the theoretical models

☐ Softwood ▨ Hardwood

Figure 2-8 Comparison between the experimental and theoretical results in terms of capacity

A significant underestimation of the load carrying capacity can be observed when the central element is made of hardwood. It is worth noting that the formulations available in literature for determining the input parameter required by the theoretical model (e.g. embedment strength, screw withdrawal capacity, screw head pull-through resistance), have been calibrated on wood species characterized by density values not exceeding 650 kg/m^3. Consequently, further studies are highly recommended in order to improve the calibration of the theoretical model.

The theoretical slip modulus ($k_{ser,th}$) was calculated by using the formulation proposed by Tomasi et al. [4]. For *fastener-to-shear plane* angles ranging between 0°≤ α ≤90°, the slip modulus was determined by considering contributions from both the axial slip modulus and the lateral slip modulus. For DT screws, the axial slip modulus was calculated considering the pull-out of the both threaded parts of the connector [31]. Otherwise, when ST screws were adopted, the axial stiffness was evaluated considering the simultaneous pull-out of the threaded part and the head penetration in the lateral timber element. In determining the lateral slip modulus, the deformation contribution from both timber elements forming the connection was taken into account by adopting the analogy of two springs placed in series (three springs when an interlayer was present). The equations and the parameters used to calculate the theoretical slip modulus are provided in the Annex B. In Figure 2-9, the comparison between the experimental and theoretical results in terms of slip modulus is reported.

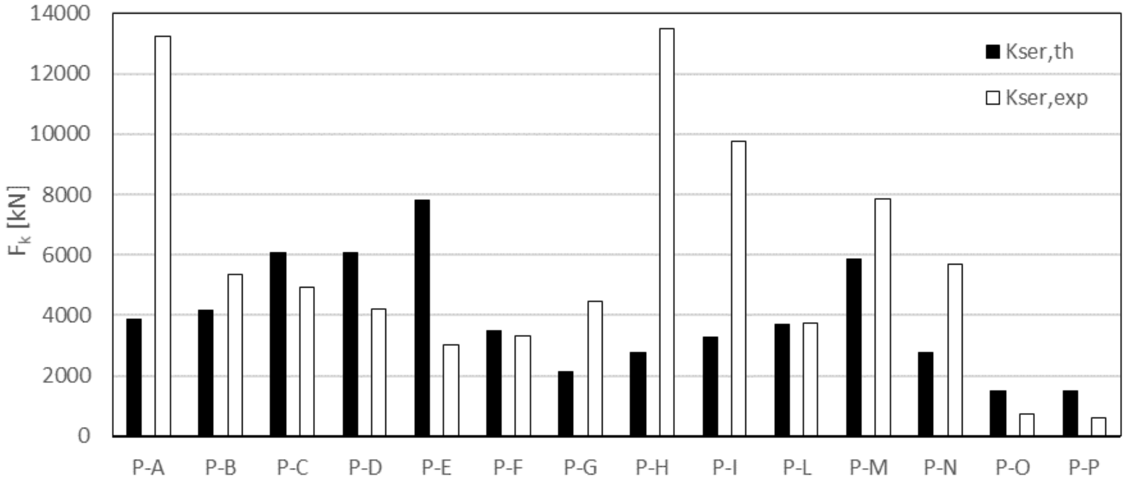

C. element	▨	▨	▨	▨	▨	☐	☐	☐	☐	☐	☐	☐	☐	☐
S. element	☐	☐	▨	▨	▨	▨	▨	▨	☐	☐	☐	☐	☐	☐
Screw	DT_A	ST_A	ST_A	ST_A	ST_A	ST_A	ST_A	DT_A	DT_A	ST_A	DT_B	ST_B	ST_B	ST_B
α	45°	45°	45°	45°	90°	45°	45°	45°	45°	45°	45°	45°	90°	90°
$K_{ser,th}$ [N/mm]	3889	4179	6053	6053	7830	3501	2145	2776	3293	3708	5862	2787	1484	1484
$K_{ser,exp}$ [N/mm]	13234	5369	4924	4192	3035	3332	4472	13468	9773	3744	7835	5700	749	616

☐ Softwood ▨ Hardwood

Figure 2-9 Comparison between the experimental and theoretical results in terms of slip modulus

Regardless of the screw-type used, the above mentioned theoretical approach (detail described in Annex B) resulted in an underestimation of the slip modulus not only for hybrid hardwood-softwood specimens with inclined screws (tests PA, PB, PF, PG and PH), but also for softwood-softwood specimens (tests PI, PL, PM, and PN). This difference appeared as more pronounced in the configurations where DT screws were adopted. This was partly attributed to uncertainties associated with the axial stiffness related to the pull-out of the threaded part of screws and the influences of the “pulling and closing effect” generated by the different thread pitch between the front thread and rear thread. Further study aimed at providing better estimations of the axial stiffness values is therefore strongly recommended.

For specimens made exclusively from hardwood (tests PC, PD and PE), a general overestimation of the slip modulus is clearly noticeable, evidencing an excessively strong sensitivity of the formulations currently available to variations in timber density values.

3 EXPERIMENTAL RESULT COMPARISON

3.1 COMPARISON PARAMETER: SCREW CONFIGURATION

As already mentioned in the introduction of this paper, studies into the influence of the fastener inclination on the mechanical behaviour of screw connections, especially as regards softwood-softwood joints connected by double threaded screws [4] and all-threaded screws [3], are available in literature. In the following, the results from the present test specimens with single threaded screws arranged in different configurations (45° - shear tension and 90°) are discussed. In particular, tests PC and PE (red curves) were made of hardwood components, while tests PN, PO and PP (black curves) were made of softwood with the interlayer previously described (Figure 3-1).

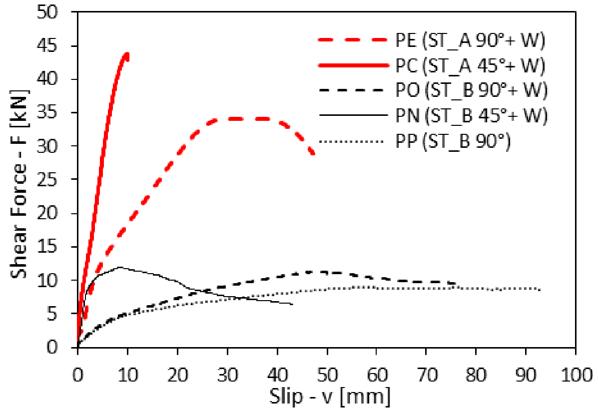

Test (connection)	$F_{max,R}$ [kN]		K_s [N/mm]	
● PE (ST_A 90°+ W)	35.03		3035	
● PC (ST_A 45°+ W)	44.95	+28%	4924	+62%
● PO (ST_B 90°+ W)	11.41		749	
● PN (ST_B 45°+ W)	12.37	+8%	5700	+661%
● PP (ST_B 90°)	9.22		616	

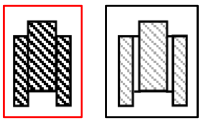

Figure 3-1 Comparisons in terms of screw configurations

Not surprisingly, significantly higher values of capacity were registered for the specimens where the hardwood was employed.

Table 3-1 Failure modes

Test	Failure mode
● PE (ST_A 90°+ W)	Splitting on the side element with formation of one plastic hinge in the screw
● PC (ST_A 45°+ W)	Tensile failure of the screw shank
● PO (ST_B 90°+ W)	Thread withdrawal with formation of two plastic hinges in the screw (rope effect)
● PN (ST_B 45°+ W)	Thread withdrawal
● PP (ST_B 90°)	Head penetration with formation of one plastic hinge in the screw (no rope effect)

As reported in Table 3-1, four different types of failure were observed. In particular, the PC tests were characterised by the tensile failure of the screw shank without significant extraction of the threaded part, while for test PN, due to the lower density of softwood, the failure was related to the thread withdrawal. As regards the 90° configurations (Figure 3-2), the maximum load in specimen PE was followed by splitting in the side elements with formation of a plastic hinge in the screw shank. In this case, the washer deformation and the high density of the panel have hindered the formation of the second plastic hinge close to the screw head. Conversely, two clearly-defined plastic hinges were observed in specimen PO. As shown in Figure 3-2, the washer reached the pull-through capacity remaining planar to the panel surface. The absence of the washer in specimen PP allowed the head penetration, thereby avoiding the formation of the second plastic hinge. As already observed in other tests [27], the impact of the rope effect on the mechanical behaviour of the connection is highlighted by comparing specimens PO and PP. In fact, the washer presence in specimen PO permitted to engage the screw withdrawal resistance, resulting in an increase of + 24% in bearing capacity. In addition, the use of washers enabled an increase of the compression force generated by the single threaded screws. As friction between the timber elements is directly proportional to the force perpendicular to the interface, a larger slip modulus (+ 22%) was registered for tests PO (with washers) compared to tests PP (without washers).

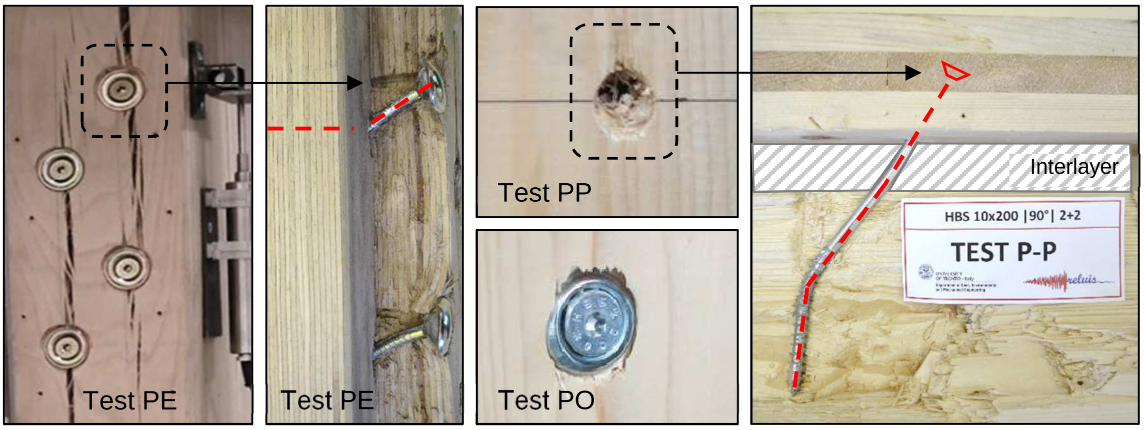

Figure 3-2 Details of 90° test configuration specimens

Unexpectedly, the slip moduli for the ST screws in 45° configurations seemed not to be positively influenced by an increase in the timber density. Actually a stiffness reduction of - 16% was observed when going from test PN (lower density) to test PC (higher density), despite the ST_B screws in PN had shorter thread length than the STA screws in PC (while similar screw head diameter). Nonetheless, all 45° configurations (for both hardwood and softwood) showed higher stiffness values than the 90° configurations where the slip modulus appeared to be highly influenced by the embedment strength of the timber elements and consequently by the material density (test PO compared to test PE).

3.2 COMPARISON PARAMETER: TIMBER PRODUCT COMBINATION (HYBRID SOLUTIONS)

In this section, the results from hybrid solutions (hardwood-softwood) will be discussed. As already mentioned, tests PF, PG and PH were realised in order to investigate the performance of connections designed for retrofit solutions of existing timber floors and therefore an interlayer of wooden boards was inserted (Figure 3-3).

As observed before, independently from the timber product arrangement, DT screws exhibited a higher stiffness, despite the smaller diameters of DT connectors (Table 2-3) with respect to the ST screws adopted.

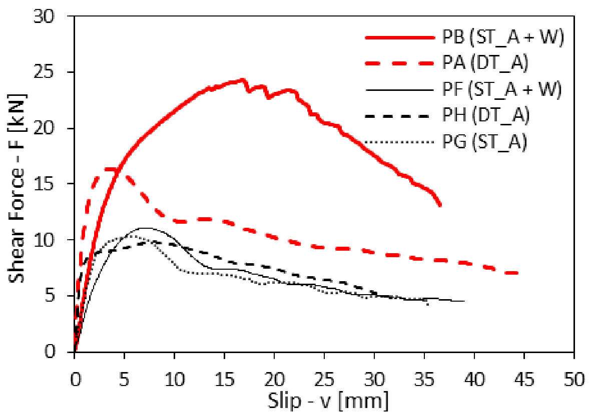

Test (connection)	$F_{max,R}$ [kN]		K_s [N/mm]	
● PB (ST_A 45°+ W)	25.34	+55%	5369	
● PA (DT_A 45°)	16.35		13234	+146%
● PF (ST_A 45°+ W)	11.13	+13%	3332	
● PH (DT_A 45°)	9.83		13468	+304%
● PG (ST_A 45°)	10.45		4472	

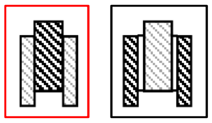

Figure 3-3 Comparisons in terms of timber hybrid configurations

When different types of timber elements are coupled, the mechanical behaviour of the connection is generally governed by the component with the lowest density value, especially regarding the failure mode. If the side element is made of hardwood (black curves), failure is strictly related to the thread withdrawal within the central element. Therefore, the maximum load depends on the geometry of the threaded part of the connector used. In this case, the resistance increase of test PF with respect to test PH (+ 13%) is comparable to the increase in the thread length (+ 11%), despite the fact that the profiles (external diameters and pitches) of the threaded parts of the two types of connectors are different. It is reasonable that the direct linear proportion between withdrawal capacity and embedment length of the threaded part in softwood [30] is reflected by the whole resistance of the connection.

Another consequence of using hardwood side elements and ST screws is that the removal of the washer (test PG compared to test PF) does not significantly affect the maximum capacity (- 6%); on the contrary, an increase in terms of slip modulus was observed (+ 34%). This might be explained by the difficulty in ensuring even contact between the bottom part of the washer (Figure 2-2-C-up) and the surface of the hardwood side element.

As regards tests PB and PA (red curves), an increase in the resistance was observed when compared to tests PF and PH. This was due to the ST_A (with washer) screws having a head pull-through resistance larger than the thread pull-out resistance (when inserted into softwood material) and DT screws having the rear-thread withdrawal capacity higher (thanks to the head presence) than the front-thread withdrawal capacity. As expected, the washer coupled with the groove cut resulted in the highest value of strength, as shown by test PB. Concerning DT screws (test PA), head pull-through was anticipated by the thread withdrawal in the side element and this explain the similar values of slip modulus of tests PA and PH. Consequently, where the side elements are made of softwood, a connection with good performance in terms of both stiffness and resistance could be obtained by increasing d_h of DT_A screws (Table 2-3).

3.3 COMPARISON PARAMETER: SCREW TYPOLOGY (ST & DT)

The performance of softwood-softwood specimens assembled with different types of screws (all inclined at a 45° angle to the grain), is compared in Figure 3-4. Due to the high pull-through resistance of the washers, both specimens employing ST screws (solid lines) failed due to thread withdrawal. Also the DT specimens (dashed lines) failed due to thread withdrawal in the central element (because of the higher capacity of the rear threaded part due to the head presence) but with maximum capacity values that are significantly lower than the values obtained from ST screws, owing to the different screw geometry (i.e. thread length and screw diameter).

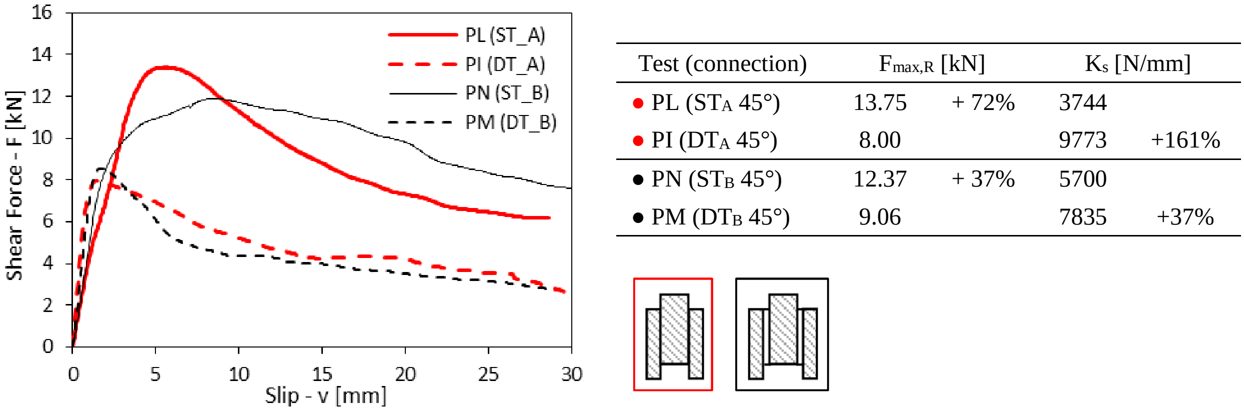

Test (connection)	$F_{max,R}$ [kN]		K_s [N/mm]	
● PL (ST_A 45°)	13.75	+ 72%	3744	
● PI (DT_A 45°)	8.00		9773	+161%
● PN (ST_B 45°)	12.37	+ 37%	5700	
● PM (DT_B 45°)	9.06		7835	+37%

Figure 3-4 Comparisons in terms of screw types

Despite the different geometry of the connectors (Figure 2-1 and Table 2-3) and the presence of the interlayer, specimens PI and PM (dashed curves) showed a similar mechanical behaviour with a failure mode strictly related to the withdrawal capacity of the threaded part inside the central element. Also in this case, as reported in Table 3-2, the extended thread length of DT_B when compared with DT_A screws (+ 14%) resulted in a higher maximum capacity (+ 13%).

Table 3-2 Characteristic axial withdrawal capacity and head pull-trough capacity from ETA (ρ_k = 350 kg/m^3)

Test	Screw	L_{t1} [mm]	D_{t1} [mm]	$f_{ax,k,45°}$ [N/mm^2]	$F_{ax,k,45°}$ [kN]	$R_{head,k}$ [kN]
PI	DT_A (L=150)	70	8	10.73	6.01	-
PM	DT_B (L=190)	80	8.2	13.35	8.76	-
PL	ST_A (L=220)	100	10	10.00	10.00	10.90
PN	ST_B (L=200)	80	10	10.64	8.51	10.75

The capacity of connections made with DT screws is maximum when the two threads are evenly inserted in the two timber elements, as the withdrawal resistance is directly related to the thread length [30]. Therefore, for applications like TTC floors where the joists and the slab have significantly different heights, the connection capacity is limited by the height of the thinner element (i.e. the slab).

A possible solution to overcome this limit could be to have uneven fasteners where the reduced length of the rear thread is balanced by an improved head pull-trough capacity (e.g. by having connectors with heads of larger sizes). However, to better understand the effects on the connection stiffness, further investigation is required.

3.4 COMPARISON PARAMETER: TIMBER PRODUCT ARRANGEMENT AND FAILURE MODE

As visible from Figure 3-5, a wide range of capacity values characterizes ST_A screws when different configurations (types of washer or the arrangement of the timber components) are considered. As showed in Figure 3-6, this can be explained by analysing the different failure modes involved.

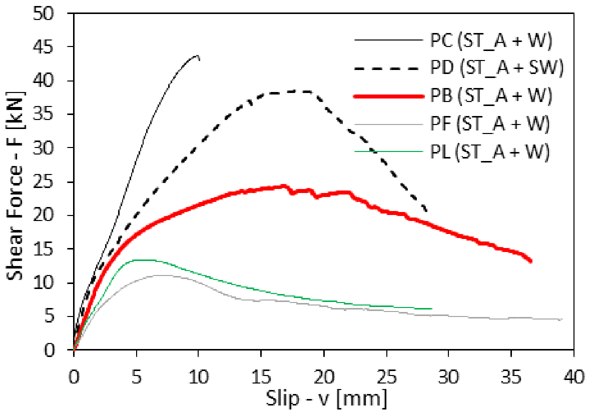

Test (connection)	$F_{max,R}$ [kN]	K_s [N/mm]	Failure mode
● PC (ST_A 45°+ W)	44.95	4924	Tensile strength
● PD (ST_A 45°+ SW)	38.91	4192	Splitting
● PB (ST_A 45°+ W)	25.34	5369	Head pull-through
● PF (ST_A 45°+ W)	11.13	3332	Thread withdrawal
● PL (ST_A 45°+ W)	13.75	3744	Thread withdrawal

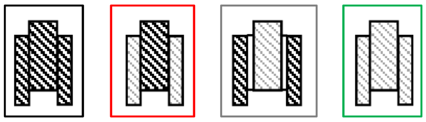

Figure 3-5 Comparisons in terms of timber configurations and failure modes

The highest resistance registered (test PC) is related to the tensile strength of the screw shank (brittle failure). For the same timber configuration but replacing the washer (W) and the groove cut with the special washer (SW), a decrease of resistance is observed. In this case, at high stress levels (force exceeding value around 35 kN), the tooth on the bottom part of the special washer (Figure 2-2-A) started to act as a knife leading to failure because of splitting in the side timber elements. As already mentioned, the lower values of resistance were obtained when the crisis involved the withdrawal capacity of the thread in the central element, independently of the type of side wooden element (tests PF and PL). It is worth mentioning that in case of failure involving thread withdrawal, the shape of the load-slip curve for slip values below 10 mm reflects the typical load-slip curve of axially loaded connectors [30]. An intermediate value of maximum capacity was registered for test PB, where pull-through failure of the washer was observed.

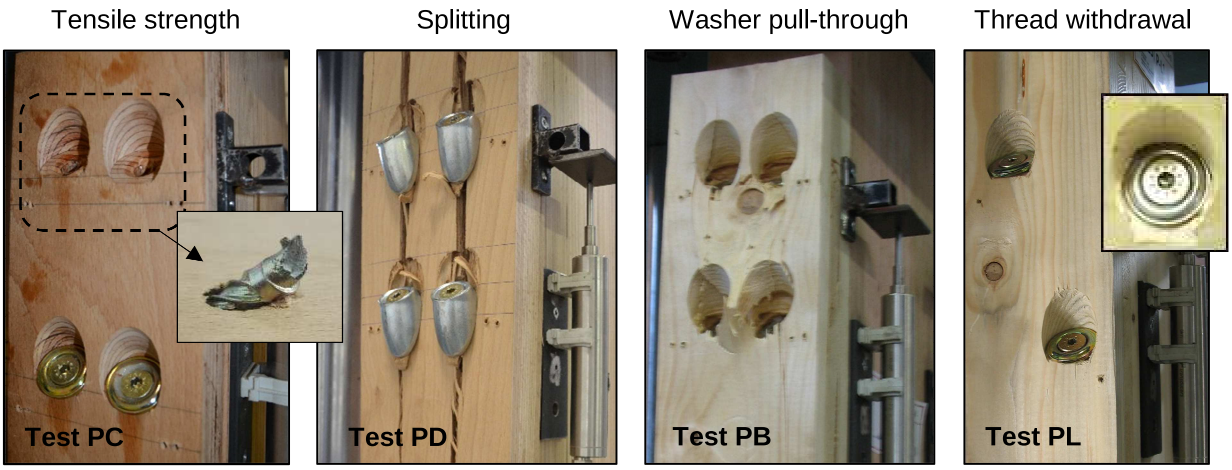

Figure 3-6 Single threaded screw: failure modes

3.5 COMPARISON PARAMETERS: DUCTILITY AND RESIDUAL STRENGTH

The values of yield slip (v_y), ultimate slip (v_u) and ductility (D) for each configuration are reported in Figure 3-7.

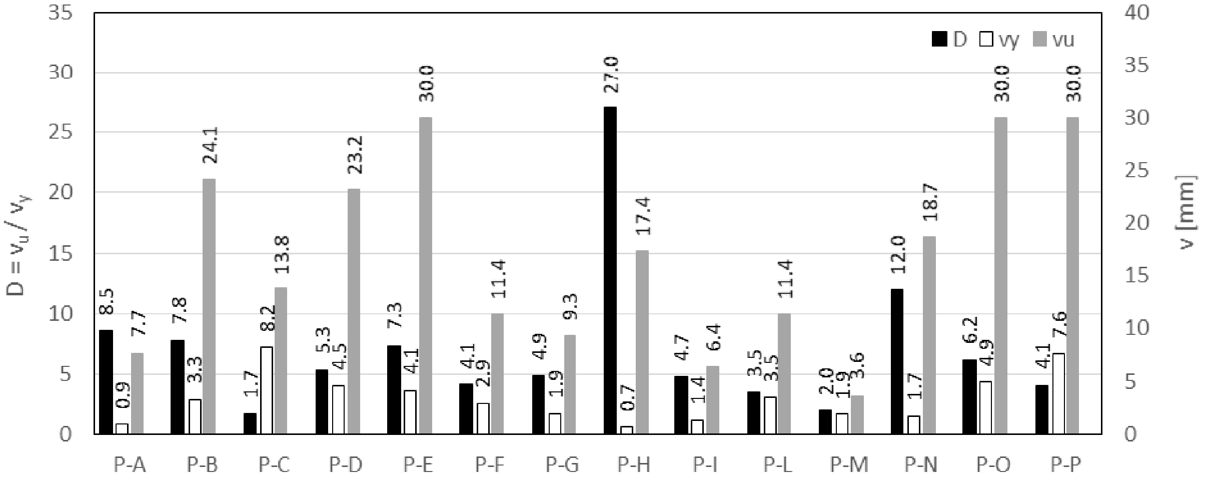

	P-A	P-B	P-C	P-D	P-E	P-F	P-G	P-H	P-I	P-L	P-M	P-N	P-O	P-P
C. element	▨	▨	▨	▨	▨	☐	☐	☐	☐	☐	☐	☐	☐	☐
S. element	☐	☐	▨	▨	▨	▨	▨	▨	☐	☐	☐	☐	☐	☐
Screw	DT$_A$	ST$_A$	ST$_A$	ST$_A$	ST$_A$	ST$_A$	ST$_A$	DT$_A$	DT$_A$	ST$_A$	DT$_B$	ST$_B$	ST$_B$	ST$_B$
L_{screw} [mm]	150	220	160	220	220	220	220	190	150	220	190	200	200	200
α	45°	45°	45°	45°	90°	45°	45°	45°	45°	45°	45°	45°	90°	90°
Washer	-	W +GC	W +GC	SW	W	W +GC	GC	-	-	W +GC	-	W +GC	W	-
Interlayer	-	-	-	-	-	20	20	20	-	-	20	20	20	20

☐ Softwood ▨ Hardwood

Figure 3-7 Experimental results in terms of yield slip, ultimate slip and ductility

The definition of ductility, described as the ratio between ultimate slip v_u and slip at yield v_y, reported in [16] gives comparable results for different timber connections only if the values of the yield slip are similar. As visible in Figure 3-7, the influence of parameters such as the screw inclination relative to the shear plane, the composition of timber members and the type of screws lead to high scattering of yield slip values. Therefore, a direct comparison between the ductility values obtained for all the tests might be misleading: for example, test PH showed the highest ductility value but it is evident that its ability to accommodate large displacements was far from being at the highest level.

The definition of an absolute ductility parameter rather than a relative one [29], such as difference $v_u - v_y$, could better represent the "ductility concept" and permit to obtain comparable results for different types of timber connections (screws, bolts, nails, etc). While the determination of ultimate slip v_u is substantially unaffected by ambiguities, the evaluation of the yield slip v_y is strongly dependent on the shape of the curve [28].

The upper bound limit of 30 mm suggested by [16] for the ultimate slip v_u, seems quite reasonable when the referenced connection is designed to be part of a hyperstatic system that most likely includes components that are incompatible with such large deformations. However, in case of screws arranged in the shear configuration ($\alpha \simeq 90°$), this 30 mm limit has a significant impact on the ductility value that is calculated. In fact, the real ultimate slip of this type of connections largely exceeds the limit (especially for softwood elements) and this causes a significant underestimation of static ductility. By analysing the results of test PE (hardwood-hardwood), it can be noted that up to slip values exceeding the 30 mm threshold, no significant force reduction was registered. In this case, a decrease of strength equal to 20 % was observed for a mean slip value of 48.61 mm (Table 3-3), associated with a ductility equal to 11.80 (+ 61 % with respect to the value calculated with an ultimate slip of 30 mm). Higher values of ductility could be obtained for tests PO and PP (softwood-softwood) where the real ultimate displacements were not registered due to the set-up limits ($v > v_{\text{max set-up}} = 90$ mm).

The post-peak behaviours of the connections are described in Table 3-3, where the mean slip values associated with a strength loss of 20, 30, 40 and 50 % are reported. For statically indeterminate structures, such data are required to determine how the load redistributes among the connectors once they have reached their peak capacity.

Table 3-3 Residual strength

$v_{Fmax,R}$	*[mm]*	3,4	17,1	11,1	16,3	33,1	6,8	5,3	7,1	1,4	5,7	1,9	10,9	47,6	70,6
$v_{0.8\ Fmax,R}$	*[mm]*	7,7	24,1	Brittle failure	23,2	48,6	11,4	9,3	17,4	6,4	11,4	3,6	18,7	$v > v_{\text{max set-up}}$	$v > v_{\text{max set-up}}$
$v_{0.7\ Fmax,R}$	*[mm]*	15,7	29,7		25,1	Specimens opening	12,8	10,6	22,0	8,3	13,0	4,8	23,2		
$v_{0.6\ Fmax,R}$	*[mm]*	21,8	33,8		26,8		19,3	18,0	27,8	11,6	16,4	5,7	32,3		
$v_{0.5\ Fmax,R}$	*[mm]*	36,6	39,6		28,1		26,3	27,7	31,4	20,9	22,0	8,7	43,5		
Test		P-A	P-B	P-C	P-D	P-E	P-F	P-G	P-H	P-I	P-L	P-M	P-N	P-O	P-P
C. element		▨	▨	▨	▨	▨	☐	☐	☐	☐	☐	☐	☐	☐	☐
S. element		☐	☐	▨	▨	▨	▨	▨	▨	☐	☐	☐	☐	☐	☐
Screw		DT_A	ST_A	ST_A	ST_A	ST_A	ST_A	ST_A	DT_A	DT_A	ST_A	DT_B	ST_B	ST_B	ST_B
L_{screw}	*[mm]*	150	220	160	220	220	220	220	190	150	220	190	200	200	200
α		45°	45°	45°	45°	90°	45°	45°	45°	45°	45°	45°	45°	90°	90°
Washer		-	W +GC	W +GC	SW	W	W +GC	GC	-	-	W +GC	-	W +GC	W	-
Interlayer		-	-	-	-	-	20	20	20	-	-	20	20	20	20

☐ Softwood ▨ Hardwood

From the comparison between tests PI with tests PM, it can be observed how the specimens having DT_A screws are characterized by a more "gentle" post-peak strength loss than the specimen realized with DT_B screws. This might be attributed to the shorter thread pitch (for both p_{t1} *and* p_{t2}) of DT_B.

It must be highlighted that all the considerations about ductility and residual strength are based on quasi-static monotonic testing. Therefore, cyclic testing is highly recommended in order to assess the behaviour of the connections under dynamic loading, especially with regard to dissipation capability.

4 CONSIDERATIONS ON PRACTICAL ISSUES

In this section, a brief discussion on practical considerations, especially regarding screw insertion into hardwood elements, is reported. According to [15], "*…for all screws in hardwoods and for screws in softwoods with a diameter d ≥ 6 mm, pre-drilling is required (the lead hole for the threaded portion should have a diameter of approximately 70 % of the shank diameter)….*" This of course increases the challenge when both elements that have to be coupled require pilot holes. To avoid problem related to precision in overlapping, both central element and side element were clamped together during pre-drilling operations.

The high temperature generated by friction during hardwood predrilling can lead to problems on drill bits, especially if long pilot holes are required (Figure 4-1). Working with TTC floors where hundreds of holes are necessary, drills and drill-bits with high performance are recommended. As an example of a suitable strategy to tackle this challenge, during the experimental campaign, grease was used for screw insertion into beech LVL elements in order to reduce friction.

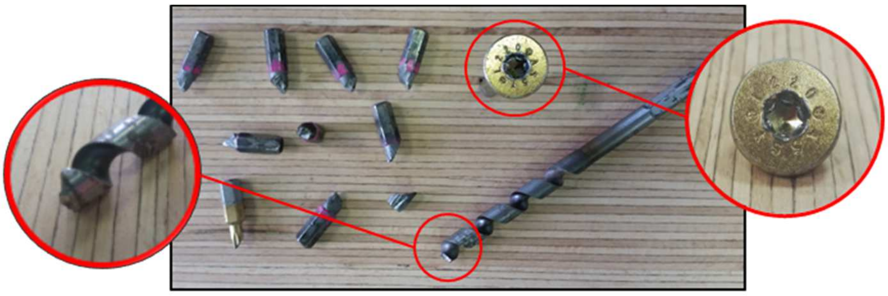

Figure 4-1 Practical issues: close up on broken insert bits, drill bits and on damaged bit-holes in screw heads

For the assembly of specimens with hardwood central elements, an impact driver was used in lieu of a "more traditional" (torque) drill. This was done in order to avoid overheating of the equipment (favoured by the particularly high torque level required to overcome friction) and to ensure a better tightening effect (i.e. to maximize the compression force developed by single thread connectors). Not rarely, the rupture of the insert drill bit occurred during the assembly phase (Figure 4-1). Damage to the bit-hole inside the screw head was also frequent.

It was demonstrated (test PF and PG) that for ST screws and hardwood side elements the use of washers is not necessary to increase connection stiffness and resistance. Therefore, the dimensions of groove cuts can be reduced or eliminated decreasing the time requested for joint fabrication.

5 FINAL REMARKS

The results of an extensive experimental campaign on timber screw connections is presented. Various timber products (i.e. softwood and hardwood in different forms: solidwood, glulam, crosslam, laminated veneer) connected by different types of screw fasteners were fabricated and tested. The most significant outcomes can be summarized as follows:

- independently of the timber product arrangements, DT screws exhibited higher stiffness than ST screws, despite having a smaller diameter (Table 2-3);
- regarding the ST screws, the shear-tension load configurations ($\alpha = 45°$) resulted in stiffer and stronger connections when compared to the shear load configuration ($\alpha = 90°$). For test arrangements with side elements made of softwood, the use of ST screws with washers permitted to obtain significantly higher values of capacity than those exhibited by DT screws in similar configurations.”
- increases in both stiffness and maximum capacity were registered for test configurations employing hardwood (i.e. hardwood-hardwood and softwood-hardwood) when compared to traditional softwood-softwood configuration. This was particularly noticeable when hardwood was used for the central element because of the inhibition of the thread withdrawal from the hardwood element;
- hardwood-hardwood specimens with inclined ST screws (45°) under shear-tension loading, failed due to tensile failure of the screw shank. The use of a connector with a larger diameter could therefore lead to an increase of the maximum capacity allowing the full exploitation of hardwood mechanical performance;
- Use of grease and an impact driver (instead of the traditional torque drill) significantly facilitates entry of the screws into engineered hardwood structural components.

ACKNOWLEDGEMENTS

The authors thank the ReLUIS-DPC network (Italian University Network of Seismic Engineering Laboratories and Italian Civil Protection Agency) for the financial support given to this study.

The authors acknowledge the financial support given to this study by the Italian Ministry of University and Research (MIUR), within the PRIN 2015 program, which funded the research "The short supply chain in the biomass-based and wood sector: supply, traceability, certification, carbon capture and storage. Innovations for green building and energy efficiency" leaded by prof. Giuseppe Scarascia Mugnozza.

Heco Italia EFG S.r.l., Pollmeier GmbH and Wurth S.r.l. are gratefully acknowledged by the authors for supplying the material used for realizing the test specimens.

NOTATIONS

The following symbols are used in this paper:

$F_{max,R}$	actual maximum load reached during test [kN]
$v_{max,R}$	connection slip corresponding to the actual maximum load reached during test [mm]
F_{15}	load corresponding to a connection slip of 15 *mm* [kN]
F'_{max}	mean maximum load according to EN 26891 [kN]
$F'_{max,i}$	maximum load of the i-*th* sample according to EN 26891 [kN]
$v_{0.1}$	connection slip corresponding to a load of $0.1 \cdot F'_{max}$ [mm]
$v_{0.4}$	connection slip corresponding to a load of $0.4 \cdot F'_{max}$ [mm]
K_s	slip modulus according to EN 26891 [N/mm]
K_{ser}	slip modulus according to EN 1995-1-1 [N/mm]
K_{lat}	lateral slip modulus (perpendicular to the screw shank) [N/mm]
K_{ax}	axial slip modulus (parallel to the screw shank) [N/mm]
F_y	yield load according to EN 12512 [kN]
v_y	yield connection slip according to EN 12512 [mm]
F_u	ultimate load according to EN 12512 [kN]
v_u	ultimate connection slip according to EN 12512 [mm]
D	ductility of connection
μ	friction coefficient for wood to wood surface

ANNEX: FORMULAS AND PARAMETERS FOR THEORETICAL VALUES CALCULATION

A: THEORETICAL LOAD-BEARING CAPACITY CALCULATION

The load-bearing capacity of the screws inserted at an angle α with respect to the shear plane (0°≤ α ≤90°) and subjected to shear-tension were calculated by adopting the model proposed by Bejtka and Blaß in [3]. As mentioned in the chapter 2.7, the following assumption was introduced: for those modes where the failure mechanism is mainly governed by the strength properties of just one of the two timber elements (i.e. modes a, b, d, e, Figure 2-7), the axial capacity of the fastener was calculated by considering only the screw-portion within the "actively involved element". Hence, for failure modes a and d, the axial capacity is the minimum between the tensile strength of the shank and the head/washer pull-through capacity (or the thread pushing-in capacity when double threaded screws are concerned). For mode b and e, the axial capacity is the minimum between the tensile strength of the shank and the thread withdrawal capacity.

The characteristic load-carrying capacity $F_{max,k,th}$ was calculated as the minimum value obtained from the following expression (see Figure 2-7):

$$R_a = R_{ax,k,1} \cdot \cos\alpha + f_{h,1,k} \cdot s_1 \cdot d_1 \cdot \sin\alpha \tag{A1}$$

$$R_b = R_{ax,k,2} \cdot \cos\alpha + f_{h,2,k} \cdot s_2 \cdot d_2 \cdot \sin\alpha \tag{A2}$$

$$\begin{aligned} R_c = R_{ax,k} \cdot (\mu \cdot \sin\alpha + \cos\alpha) + \frac{f_{h,1,k} \cdot s_1 \cdot d_1}{1+\beta}\left(1 - \frac{\mu}{\tan\alpha}\right)\left[\sqrt{\beta + 2\beta^2\left[1 + \frac{s_2}{s_1} + \left(\frac{s_2}{s_1}\right)^2\right] + \beta^3\left(\frac{s_2}{s_1}\right)^2} - \right. \\ \left. -\beta\left(1 + \frac{s_2}{s_1}\right)\right] \end{aligned} \tag{A3}$$

$$R_d = R_{ax,k,1} \cdot (\mu \cdot \sin\alpha + \cos\alpha) + \frac{f_{h,1,k} \cdot s_1 \cdot d_1}{2+\beta}\left(1 - \frac{\mu}{\tan\alpha}\right)\left[\sqrt{2\beta(1+\beta) + \frac{4\beta \cdot (2+\beta) \cdot M_{y,k} \cdot sin^2\alpha}{f_{h,1,k} \cdot d_1 \cdot s_1^2}} - \beta\right] \tag{A4}$$

$$R_e = R_{ax,k,2} \cdot (\mu \cdot \sin\alpha + \cos\alpha) + \frac{f_{h,1,k} \cdot s_2 \cdot d_2}{1+2\beta}\left(1 - \frac{\mu}{\tan\alpha}\right)\left[\sqrt{2\beta^2(1+\beta) + \frac{4\beta \cdot (1+2\beta) \cdot M_{y,k} \cdot sin^2\alpha}{f_{h,1,k} \cdot d_2 \cdot s_2^2}} - \beta\right] \tag{A5}$$

$$R_f = R_{ax,k} \cdot (\mu \cdot \sin\alpha + \cos\alpha) + \left(1 - \frac{\mu}{\tan\alpha}\right)\sqrt{\frac{2\beta}{1+\beta}}\sqrt{2 \cdot M_{y,k} \cdot f_{h,1,k} \cdot d_1 \cdot sin^2\alpha} \tag{A6}$$

Where α is the *fastener-to-shear plane* angle; μ is the friction coefficient for wood-to-wood surfaces assumed as equal to 0.25; s_i is the anchorage length of the screw inserted into element; d_i is the effective diameter of the screw part inserted into timber element (d_{shank} for ST screws; $1.1 \cdot d_{core}$ for DT screws); $f_{h,i,k}$ is the characteristic embedment strength of the relative timber element; $\beta = f_{h,2,k}/f_{h,1,k}$; and $M_{y,k}$ is the characteristic yield moment of the screw. In the absence of experimental data, $M_{y,k}$ was determined according to the relevant technical approval (see Table 2-3). $R_{ax,k,1}$ is the axial resistance of the screw part inserted in the lateral timber element. For ST screws, $R_{ax,k,1}$ was assumed as equal to the minimum value between the characteristic head pull-through resistance ($R_{head,k}$) and the characteristic tensile strength of the screw ($R_{tens,k}$). Otherwise, for DT screws, $R_{ax,k,1}$ was assumed as equal to the minimum value between the characteristic thread withdrawal resistance ($R_{thread,k}$) and the characteristic tensile strength of the screw ($R_{tens,k}$). $R_{ax,k,2}$ is the axial resistance of the screw part inserted in the central timber element, corresponding to the minimum value between the characteristic thread withdrawal resistance ($R_{thread,k}$) and the characteristic tensile strength of the screw ($R_{tens,k}$). As regards equations (A3) and (A6), $R_{ax,k} = min\{R_{ax,k,1}; R_{ax,k,2}\}$.

Every term in equations (A1) - (A6) was determined according to the provisions contained in the relevant product certificate ([22],[23],[24] and [25]). When missing, the formulations reported in the Eurocode 5 [15] were used.

When considering connections comprising hardwood elements, in the absence of specific indications from the literature, the thread withdrawal capacity ($R_{thread,k}$) and the head-pull through capacity ($R_{head,k}$) were considered to be greater than the tensile strength of the screws to better represent the experimental behaviour (e.g. brittle failure of the screw shank registered in P-C test).

The results of the theoretical load-bearing capacity calculation are summarized in Table A-1:

Table A-1 Theoretical load-bearing capacity calculation

	P-A	P-B	P-C	P-D	P-E	P-F	P-G
$R_{ax,k,1}$ [kN]	6,76	10,89	26,00	26,00	26,00	26,00	26,00
$R_{ax,k,2}$ [kN]	18,00	26,00	26,00	26,00	26,00	10,00	10,00
$f_{h,1,k}$ [N/mm^2]	15,01	15,22	25,66	25,66	44,90	25,66	25,66
$f_{h,2,k}$ [N/mm^2]	25,43	24,88	24,88	24,88	43,54	14,76	14,76
$M_{y,k}$ [Nmm]	20000	36000	36000	36000	36000	36000	36000
$F_{max,k,th}$ [kN]	**7,06**	**11,28**	**23,61**	**23,61**	**11,29**	**10,49**	**10,49**

	P-H	P-I	P-L	P-M	P-N	P-O	P-P
$R_{ax,k,1}$ [kN]	18,00	6,76	10,89	9,51	10,75	10,75	3,50
$R_{ax,k,2}$ [kN]	8,18	6,36	10,00	8,76	8,51	9,36	9,36
$f_{h,1,k}$ [N/mm^2]	25,30	15,01	15,22	14,94	15,25	26,69	26,69
$f_{h,2,k}$ [N/mm^2]	15,09	15,09	14,76	15,06	14,76	25,83	25,83
$M_{y,k}$ [Nmm]	20000	20000	36000	19500	35830	35830	35830
$F_{max,k,th}$ [kN]	**8,32**	**6,59**	**10,32**	**8,73**	**8,98**	**5,97**	**4,50**

B: THEORETICAL SLIP MODULUS CALULATION

In order to evaluate the slip modulus of the connections where the screws were inserted at an angle α with respect to the shear plane (0°≤ α ≤90°), the formulation proposed by Tomasi et al. [4] was used:

$$K_{ser} = K_{lat} \cdot \sin\alpha\,(\sin\alpha - \mu \cdot \cos\alpha) + K_{ax} \cdot \cos\alpha\,(\cos\alpha - \mu \cdot \sin\alpha) \tag{B1}$$

Where K_{lat} and K_{ax} are, respectively, the axial and lateral slip moduli of the screw connection and μ is the friction coefficient for wood to wood surfaces assumed as equal to 0.25.

The axial slip modulus K_{ax} of the DT screws was calculated considering the simultaneous pull-out of the two threaded parts of the connector as proposed by Kevarinmäki [31]. By analogy with the behaviour of two springs placed in series, the axial slip modulus can be calculated as followed:

$$K_{ax} = \frac{1}{1/K_{ax,1} + 1/K_{ax,2}} \tag{B2}$$

The same equation was employed for the connections where ST screws were used. In this case, $K_{ax,2}$ corresponds to the axial stiffness due to the head penetration in the lateral timber and $K_{ax,1}$ is the axial stiffness of the threaded part of the connector.

The axial stiffness related to the pull-out of the threaded part of screws was calculated as:

$$K_{ax,i} = c_1 \cdot d_i^{c_2} \cdot l_{ef,i}^{c_3} \tag{B3}$$

Where d is the outer thread diameter and l_{ef} is the penetration length of the threaded part into the timber member. The coefficients c_1, c_2 and c_3 were assumed according to the relevant technical approvals ([22],[23],[24] and [25]).

Due to the lack of specific indications for evaluating the axial slip modulus associated with the ST head penetration into the lateral timber member tentative equation (B4) was used:

$$K_{ax} = E_\alpha \frac{\pi \cdot d_h^2 \cdot \sin\alpha}{4 \cdot t_{side}} \tag{B4}$$

Where d_h is the diameter of the screw head (or diameter of the washer when adopted), α angle between the screw axis and the grain, t_{side} is the thickness of the lateral timber member and E_α is the modulus of elasticity along direction α with respect to the grain. The criterion proposed by Hankinson [32] was used:

$$E_\alpha = \frac{E_0 \cdot E_{90}}{E_0 \cdot sin^2\alpha + E_{90} \cdot cos^2\alpha} \tag{B5}$$

The lateral slip modulus K_{lat} was evaluated by considering the deformation occurring in both timber elements through the following relation:

$$K_{lat} = \frac{1}{1/K_{lat,1} + 1/K_{lat,2}} \tag{B6}$$

Where $K_{lat,1}$ and $K_{lat,2}$ are the lateral slip moduli (perpendicular to the screw shank) relative to the deformation of the single timber components. The lateral slip modulus was calculated as:

$$K_{lat,i} = 2\left(\rho_m^{c_4} \cdot \frac{d^{c_5}}{c_6}\right) \tag{B7}$$

Which is consistent with the formulation recommended by EN 1995-1-1 [15] for steel-to-timber and concrete-to-timber connections (where the fastener part embedded into the concrete is assumed as rigid). It is worth noting that in cases where the two timber components are made from the same timber material, K_{lat} (B6) becomes equal to K_{ser} [15]. The coefficients c_4, c_5 and c_6 were assumed in accordance with Table 7.1 of [15].

For tests PF, PG, PH, PN, PO, PP and PP where an interlayer made of timber boards was present, the lateral slip modulus K_{lat} was evaluated by considering the deformation of three separate contribution:

$$K_{lat} = \frac{1}{1/K_{lat,1} + 1/K_{int} + 1/K_{lat,2}} \tag{B8}$$

Where the lateral slip modulus relative to the interlayer was calculated as:

$$K_{int} = \rho_m^{c_4} \cdot \frac{d^{c_5}}{c_6} \tag{B9}$$

The results of the theoretical slip modulus calculation are summarized in Table B-1:

Table B-1 Theoretical slip modulus calculation

	P-A	P-B	P-C	P-D	P-E	P-F	P-G
K_{ax} [N/mm]	3253	3848	4987	4987	-	4574	2404
K_{lat} [N/mm]	4948	4730	7830	7830	7830	1712	1712
K_{ser} [N/mm]	**3889**	**4179**	**6053**	**6053**	**7830**	**3501**	**2145**

	P-H	P-I	P-L	P-M	P-N	P-O	P-P
K_{ax} [N/mm]	3598	3253	3848	8536	3569	-	-
K_{lat} [N/mm]	1406	3359	3474	1405	1484	1484	1484
K_{ser} [N/mm]	**2776**	**3293**	**3708**	**5862**	**2787**	**1484**	**1484**

REFERENCES

[1] Dietsch F., Brandner R. (2015) Self-tapping screws and threaded rods as reinforcement for structural elements. Construction and Building Materials, 97. 78 – 89.

[2] Loss C., Piazza M., Zandonini R. (2016) Connections for steel–timber hybrid prefabricated buildings. Part I: Experimental tests. Construction and Building Materials, 122. 781 – 798.

[3] Bejtka I., Blass H. J. (2002) Joints with inclined screws. In: Proceedings from meeting thirty-five of the international council for building research studies and documentation, CIB, Working Commission W18 – Timber Structure, Kyoto, Japan.

[4] Tomasi R., Crosatti A., Piazza M. (2010) Theoretical and experimental analysis of timber-to-timber joints connected with inclined screws. Construction and Building Materials 24, pages: 1560 – 1571.

[5] Giongo I., Schiro G., Piazza M., Tomasi R. (2016) Long-term out-of-plane testing of timber floors strengthened with innovative timber-to-timber solutions. Proceedings of the World Conference on timber Engineering (WCTE), Vienna, Austria.

[6] Ozarska B. (1999) A review of the utilization of hardwoods for LVL. Wood Science and Technology, 33. 341-351.

[7] Aicher S., Christian Z., Dill-Langer G. (2014) Hardwood glulams – emerging timber products of superior mechanical properties. Proceedings of the World Conference on timber Engineering (WCTE), Quebec City, Canada.

[8] Knorz M., Van de Kuilen J.W. (2012) Development of a high-capacity engineered wood product – LVL made of European Beech. Proceedings of the World Conference on timber Engineering (WCTE), Auckland, New Zealand.

[9] Misconel A., Ballerini M., Van de Kuilen J.W. (2016) Steel-to-timber joints of beech-LVL with very high strength steel dowels. Proceedings of the World Conference on timber Engineering (WCTE), Vienna, Austria.

[10] Kobel P., Steiger R., Frangi A. (2014) Experimental analysis on the structural behaviour of connections with LVL made of Beech wood. In Materials and Joints in Timber Structures, RILEM Bookseries 9, Springer, pages: 211 – 220.

[11] Celebi G., Kilic M. (2007) Nail and screw withdrawal strength of laminated veneer lumber made up hardwood and softwood layers. Construction and Building Materials, 21. 894–900.

[12] Ali Taj M., Najafi S. K., Ebrahimi G. (2009) Withdrawal and lateral resistance of wood screw in beech, hornbeam and poplar. European Journal of Wood and Wood Products, 67. 135-140. DOI 10.1007/s00107-008-0294-9.

[13] Sebastian W., Mudie J., Cox G., Piazza M., Tomasi R., Giongo I. (2016) Insight into mechanics of externally indeterminate hardwood–concrete composite beams. Construction and Building Materials, Volume 102, Part 2, pages: 1029 – 1048.

[14] Johansen KW. (1949) Theory of timber connections. International association of bridge and structural engineering. Bern, Volume 9, pages 249 – 262.

[15] European Committee for Standardization (2014). EN 1995-1-1:2004+A2:2014: Eurocode 5 - Design of timber structures, Part 1-1, General - Common rules and rules for buildings. CEN, Brussels, Belgium

[16] European Committee for Standardization (2001). EN 12512: Timber structures – Test methods – Cyclic testing of Joints made with mechanical fasteners. CEN, Brussels, Belgium.

[17] European Committee for Standardization (1991). EN 26891: Timber structures – Joints made with mechanical fasteners – General principles for the determination of strength and deformation characteristics. CEN, Brussels, Belgium.

[18] ETA (European Technical Approval) 14/0354: Glued laminated timber made of hardwood – Structural laminated veneer lumber made of beech.

[19] European Committee for Standardization (2009). EN 338: Structural timber – Strength classes. CEN, Brussels, Belgium.

[20] Certificate of performance No. 0672-CPR-0415 (MPA Stuttgart 0672).

[21] ETA (European Technical Approval) 12/0347: X-Lam Dolomiti – CLT.

[22] ETA (European Technical Approval) 11/0190: Würth self-tapping screws.

[23] ETA (European Technical Approval) 11/0030: Rotho Blaas self-tapping screws

[24] ETA (European Technical Approval) 12/0121: HECO-TOPIX-T and HECO-TOPIX-CC self-tapping screws.

[25] ETA (European Technical Approval) 12/0063: SFS self-tapping screws WT

[26] European Committee for Standardization (2005). EN 1990:2002+A1:2005: Eurocode - Basis of structural design. CEN, Brussels, Belgium.

[27] Ballerini M. (2012) Experimental investigation on parallel-to-grain wood-to-wood joints with self-tapping screws. Proceedings of the World Conference on timber Engineering (WCTE), Auckland, New Zealand.

[28] Piazza M., Polastri A., Tomasi R. (2011) Ductility of timber joints under static and cyclic loads. Proceedings of the Institutional of Civil Engineers, Structures and buildings 164 April 2011 Issue SB2, pages: 79 - 90.

[29] Jorissen A., Fragiacomo M. (2011) General notes on ductility in timber structures. Engineering Structures. Volume 33, Issue 11, pages 2987-2997.

[30] Stamatopoulos H., Malo K.A. (2015) Withdrawal capacity of threaded rods embedded in timber elements. Construction and Building Materials 94, pages: 387 – 397.

[31] Kevarinmäki A. (2002) Joints with inclined screws. Proceedings of meeting thirty-five of the international council for building research studies and documentations, CIB, Working Commission W18 – Timber Structures, Kyoto, Japan.

[32] Hankinson. R. L. (1921) Investigation of crushing strength of spruce at varying angles of grain. Air Service Information Circular No. 259, U.S. Air Service.